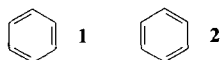


Communications may be submitted in English or in German. Further details regarding the submission of communications can be found in the "Notice to Authors" reproduced in the January issue of the journal. Copies thereof may be obtained from the editorial office upon request.

## A New Look at Electron Localization\*\*

By A. Savin,\* A. D. Becke, J. Flad, R. Nesper, H. Preuss and H. G. von Schnering

Ubiquitous chemical terms such as "the electron pair" and "the chemical bond" do not correspond unambiguously to directly measurable physical quantities. Because of their undeniable conceptual utility, however, clear and rigorous physical definitions are essential. The chemical bond is often described by localized molecular orbitals (see for example ref. [1]), but localized orbital sets are not unique. For example, two possibilities for bond localization of the  $\pi$  orbitals in benzene are shown in **1** and **2**, yet other, indeed infinitely many, mathematically equivalent schemes are also possible.<sup>[2]</sup> The localized molecular orbital description of chemical bonding is physically and mathematically arbitrary.



In this work it will be demonstrated, through a series of examples, that a new quantity, the Electron Localization Function (ELF),<sup>[3]</sup> is especially well suited to describe chemical bonds and electron pairs. ELF is based on measurable quantities and, moreover, the problem of nonuniqueness of localized molecular orbitals is not shared by ELF, at least in closed-shell systems.

In 1952 Lennard-Jones had already shown how, with the help of quantum mechanics, regions of space could be related to bonds and lone electron pairs.<sup>[4]</sup> He employed the

two-particle density for electrons of parallel spin, a function of two electrons' coordinates ( $x, y, z$  and  $x', y', z'$ ) which gives the joint probability of finding one electron at position  $x, y, z$  and another electron of the same spin at position  $x', y', z'$ . The analysis showed that electrons of parallel spin restrict themselves to separate regions of space, and hence follows the notion of localized electron pairs. A well-known application of these concepts are the Gillespie and Nyholm rules.<sup>[5]</sup>

Becke and Edgecombe investigated another way of defining such regions of electron localization. They likewise made use of the two-electron density, exploiting its behavior at small interelectronic distances.<sup>[3]</sup> They showed that the probability of finding two electrons of the same spin close to one another is highly position dependent, leading to regions of both particularly high and particularly low pair probability. In the latter case, the electrons are "well localized". As a measure of this, Becke and Edgecombe introduced the Electron Localization Function (ELF), defined so as to have the convenient range of values  $0 \leq \text{ELF} \leq 1$ . Regions in which the value of ELF is close to 1 correspond to well-localized electrons, and may be identified with atomic shells, chemical bonds and lone electron pairs. It is remarkable that the behavior of only the parallel-spin electrons so clearly discerns these details. The nature of electron pair correlation for opposite spins will not be considered here.

*Technical details:* Let us consider two electrons with parallel spins at positions  $x, y, z$  and  $x', y', z'$  (with separation  $r_{12}$ ). The two-particle density is a function of both  $x, y, z$  and  $x', y', z'$ . Upon averaging over a sphere centered on  $x, y, z$ , one obtains a function of  $x, y, z$  and  $r_{12}$ , whose power series in  $r_{12}$  has the leading term  $D(x, y, z)r_{12}^2$ . The definition of ELF is then given by equation (a), where  $D_h(x, y, z)$  is the value of  $D$  for a homogeneous electron gas with

$$\text{ELF} = \frac{1}{1 + [D(x, y, z)/D_h(x, y, z)]^2} \quad (\text{a})$$

density  $\rho(x, y, z)$ . In the Hartree-Fock approximation (closed shell) one obtains the explicit expression given in equation (b), where  $\phi_i$  are the occupied orbitals

$$D/D_h = 0.3483 \rho^{-5/3} \left[ \sum_i |\nabla \phi_i|^2 - \frac{1}{8} |\nabla \rho|^2 / \rho \right] \quad (\text{b})$$

and all quantities are expressed in atomic units. In this work, ELF has been calculated at the Hartree-Fock level [6], with pseudopotentials used for the tin compounds [7].

It is, in principle, possible to determine ELF from measured data. Knowledge of only the single-particle density matrix  $\sum_i \phi_i(r)\phi_i(r')$  is required at the Hartree-Fock level and methods to determine this from experimental data have been proposed long ago [8]. In many cases the experimental electron density was used to determine the density matrix. Knowledge of the density should be supplemented, however, by additional information from sources such as Compton spectroscopy [9, 10].

Here we present, using a newly developed computer graphics program,<sup>[11]</sup> the first extensive study of the utility of the Electron Localization Function. In the graphical representations of Figure 1, we see how well ELF reflects various intuitive concepts of atomic and molecular structure. The program calculates both the electron density and ELF for selected molecular planes, which generally contain atomic nuclei, and portrays them simultaneously. Electron density is represented by point density (i.e., electron clouds) as, for

[\*] Dr. A. Savin, Prof. Dr. R. Nesper[<sup>†</sup>], Prof. Dr. H. G. von Schnering  
Max-Planck-Institut für Festkörperforschung  
Heisenbergstrasse 1, W-7000 Stuttgart 80 (FRG)

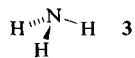
Dr. J. Flad, Prof. Dr. H. Preuss  
Institut für Theoretische Chemie, Universität Stuttgart  
Pfaffenwaldring 55, W-7000 Stuttgart 80 (FRG)

Prof. Dr. A. D. Becke  
Department of Chemistry, Queen's University  
Kingston, Ontario K7L 3N6 (Canada)

[\*\*] This work was supported by the Fonds der Chemischen Industrie, the Deutsche Forschungsgemeinschaft, the Höchst AG (Frankfurt), the Bundesministerium für Forschung und Technologie and the Natural Sciences and Engineering Research Council of Canada. We thank F.-X. Fraschio, M. Kohout and B. Miehlich (Universität Stuttgart) for the assistance with the computer graphics. We are indebted to Prof. P. Fulde (Stuttgart) and Prof. W. H. E. Schwarz (Siegen) for valuable suggestions.

[<sup>†</sup>] New address: Laboratorium für Anorganische Chemie der Eidgenössischen Technischen Hochschule, Zürich

example, in Frame 1 for the electron density of the  $\text{NH}_3$  molecule, 3. With white points on a black background, one



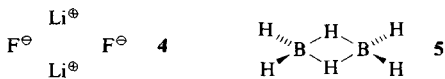
immediately recognizes the high-density maxima at the positions of the N nucleus and the H nucleus. Representations of this kind were introduced in 1931.<sup>[12]</sup>

In addition our points are assigned colors depending on the local value of ELF and inspired by geographical maps: the blue color of the sea corresponds to low ELF and the white of the mountains to high ELF, with green and brown in between. The color scale is given on the left in Frame 2. Thus our backgrounds remain black, and white points now indicate very highly localized electrons. This representation of ELF conveys considerable additional information. One now identifies in 3, for instance (compare Frames 1 and 2), three regions of higher localization: one around the N nucleus, one containing the N and H atoms (lower right) and one on the free side of the N atom (top). These regions can be attributed to the core, the N–H bond and the lone pair.

At this stage it should be pointed out that the Electron Localization Function, like the electron density, always possesses the full symmetry of the molecule, and therefore all symmetry-equivalent planes will give the same ELF. For  $\text{NH}_3$  (3) all planes containing the  $C_3$  axis and one of the N–H bonds will yield the same picture. Furthermore for linear molecules both the electron densities and ELF have axial symmetry. In the case of the Ne atom, ELF yields two spherical regions of higher localization which correspond to the core and valence shells (Frame 3). The same sharp separation between core and valence shells is also visible in molecules such as  $\text{Li}_2$  (Frame 4).

In the  $\text{C}_2$  molecule ( $1^1\Sigma_g^+$  state) the  $\pi$ -orbital bonding is discernible (Frame 5). In the  $\text{N}_2$  molecule there exists within the valence shell a clear separation between the bonding region and the lone pair electrons, not as distinct, however, as the separation between core and valence regions (Frame 6). The  $\text{F}_2$  molecule (Frame 7) shows a weak bond, whereas two Ne atoms at the same interatomic distance merely show a distortion of their valence shells (Frame 8).

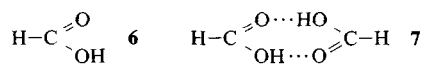
Even with simple hydrides we find a large variety of bonding forms. The LiH molecule consists of a  $\text{Li}^\oplus$  core (Frame 9, left) and a polarized  $\text{H}^\ominus$  ion (right, white). In the BH molecule (Frame 10, B middle, H right) there exists along with the B–H bond an additional electron lone pair (left). In the HF molecule (Frame 11) the region of space to which one would assign the H–F bond is smaller and more difficult to discern from the region of the free electrons than in, for example, the BH molecule. We see already an indication of the tendency to form  $\text{H}^\oplus\text{F}^\ominus$ . In the LiF molecule we have essentially an ionic bond (Frame 12; compare with LiH,



Frame 9), as implied by the nearly spherical structure of the ELF around each nucleus and the appearance of an intervening region with very low ELF values. This ionic character also appears, of course, in the dimer  $\text{Li}_2\text{F}_2$  (4, Frame 13). In contrast, a polarized bond is found in the ClF molecule (Frame 14).

The more complicated case of three-center bonding appears in diborane (5, Frame 15). Here also, the agreement with classical concepts is very clearly illustrated by the electron density and ELF. In planar  $\text{Li}_4$  and  $\text{Li}_6$  clusters, calculated to be stable, the three-center bonds likewise appear.<sup>[6]</sup> In these cases, however, one might also expect bonds involving more than three centers. According to ELF (Frames 16 and 17), these clusters are held together almost exclusively by peripheral three-center bonds.

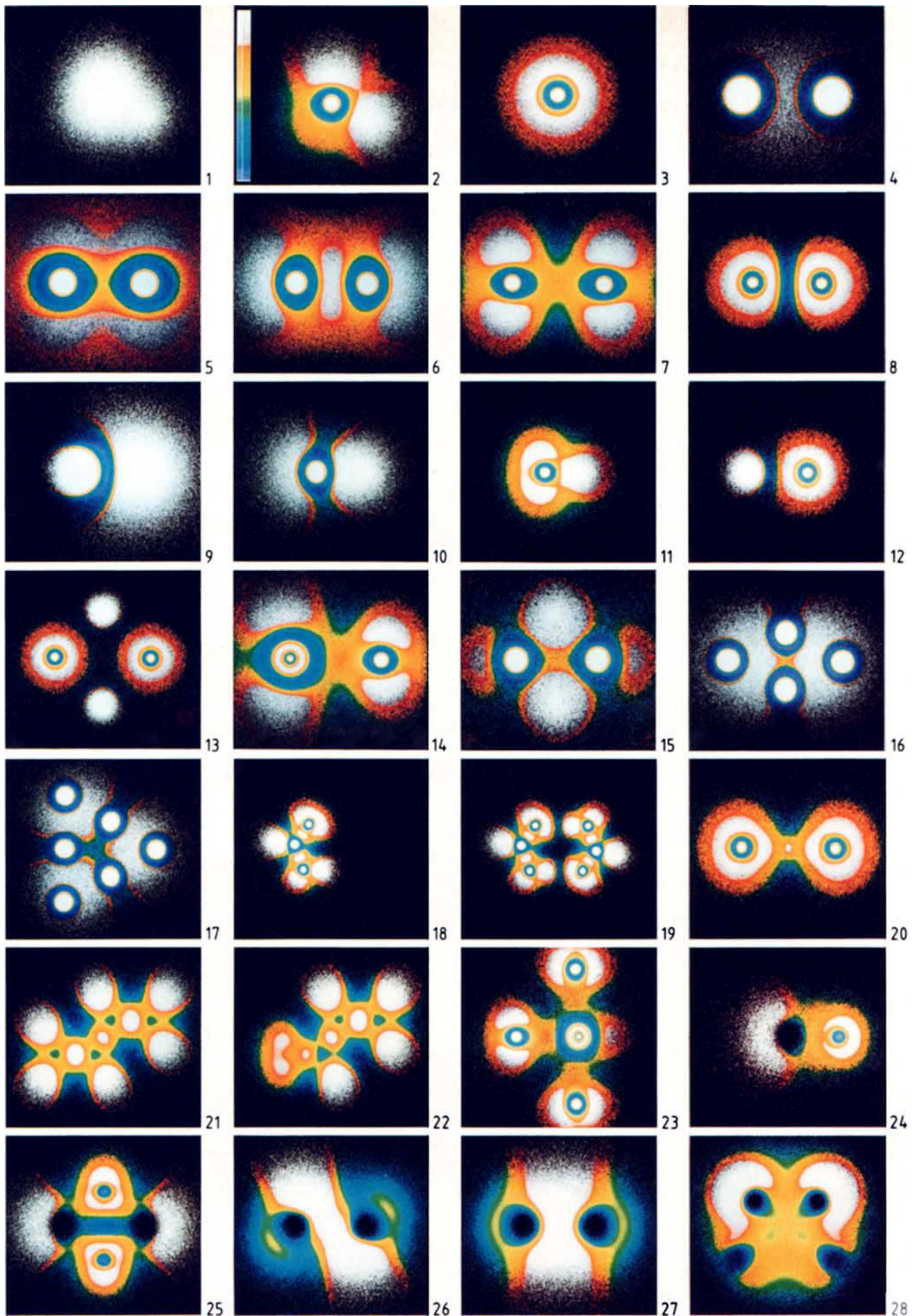
When H bridges two strongly electronegative partners the bonds show distinct ionic character, as indicated by the formic acid molecule 6 (Frame 18) and its dimer 7 (Frame 19). What happens, though, if the H atom lies symmetrically



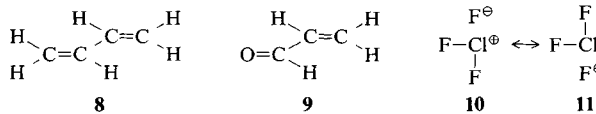
between two equally electronegative atoms as in the FHF anion (Frame 20)? Here one notices a region of high ELF around the proton clearly separated from those of the neighboring atoms. A similar picture results if, in 7, one imagines the transition state for the transfer of a proton from one O atom to another. In the change from an asymmetric to a symmetric H bridge the ionic nature of the bond is largely lost.

With the Electron Localization Function weaker effects, such as change in delocalization, can also be recognized. Let

Fig. 1. Electron density  $\rho$  as "cloud" and the color pattern of the Electron Localization Function, ELF (scale in Frame 2: small values of the ELF are represented as blue, large values as white; scale for remaining frames: blue, green, brown, white; background: black). Frame 1:  $\rho(3)$  as white cloud. The selected plane contains the N nucleus (middle), a H nucleus (bottom right) and the center point between two other H nuclei. Frame 2:  $\rho(3)$  and the ELF. The white regions correspond to the core, the lone electron pair and the N–H bond. Frame 3: Core and valence shells of the Ne atom. Frame 4: Core and bonding regions (white) in the  $\text{Li}_2$  molecule. Frame 5: Core and  $\pi$  bond (white periphery) in the  $\text{C}_2$  molecule. Frame 6: Core, bond and lone electron pair (white) in the  $\text{N}_2$  molecule. Frame 7: Core, cylindrical symmetric regions of the lone electron pair (white) and weak covalent bond (yellow-brown) in the  $\text{F}_2$  molecule. Frame 8: Deformation of the electron density in the  $\text{Ne}_2$  molecule (compare Frame 3). Frame 9: LiH molecule with  $\text{Li}^\oplus$  core (left) and  $\text{H}^\ominus$  ion (right). Frame 10: BH molecule with the lone electron pair, the B core and the B–H bond as white regions from left to right. Frame 11: HF molecule with the cylindrical symmetric regions of the lone electron pair, the F core and the F–H bond. Frame 12: LiF molecule with  $\text{Li}^\oplus$  (left) and  $\text{F}^\ominus$  (right). Model for an ion pair with separated region (small ELF values: blue). Frame 13: 4 with  $\text{Li}^\oplus$  cations (top and bottom) and  $\text{F}^\ominus$  anions (left and right). Frame 14: ClF molecule with Cl (left) and F (right); core and lone electron pair regions (large white regions); weak, polarized bond (brown-yellow region). Frame 15: 5 (plane of the  $\text{B}_2\text{H}_2$  ring with the B atoms left and right) with core and two three-center bonds (large white regions around the H atoms). Frame 16: Planar  $\text{Li}_4$  cluster with core and two three-center bonds. Frame 17: Planar  $\text{Li}_6$  cluster with core and three peripheral three-center bonds; one notices that a central three-center bond is absent. Frame 18: 6 with cores, bonds and lone electron pairs (ketone oxygen at top right). Frame 19: 7 (compare Frame 18) shows the ionic character of the hydrogen bonds (blue regions between the monomers). Frame 20: FHF $^\ominus$  ion with a small area of high ELF values around the H nucleus. Frame 21: 8 (selected plane is 1 Bohr above the nuclear plane) with the C–H and C–C bonds (white regions). Frame 22: 9 (plane same as in Frame 21) shows a larger  $\pi$  region at the central C–C bond than 8. Frame 23: ClF $_3$  molecule emphasizing the difference between the axial and equatorial Cl–F bonds. Frame 24: SnO molecule with Sn (left) and O (right) and the lone electron pair on the Sn (large white region). Frame 25:  $\text{Sn}_2\text{O}_2$  molecule with the Sn atoms lying horizontally. Frame 26: 12 (plane through the Sn nuclei splits the H–Sn–H angle; the H nuclei are located top right and bottom left above and below the plane), see text for discussion. Frame 27:  $\text{Sn}_2\text{H}_2$  molecule with hypothetical planar structure (Sn atoms sit right and left from the center point of the picture: all H atoms are located in a plane perpendicular to the represented plane). Frame 28:  $\text{Cu}_2\text{Sn}_4$  molecule with heterocubane structure (Sn atoms top, Cu atoms bottom), for discussion see text.

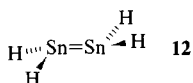


us compare the C–C bonds in butadiene (**8**, Frame 21), and acrolein (**9**, Frame 22). The illustrations present ELF values in a plane lying 1 Bohr above the plane of the nuclei and intersecting the  $\pi$ -bonding region, and show that the  $\pi$  component of the C–C bond is larger in **9** than it is in **8**.



That ELF also represents three-center–four-electron bonds is shown by the example of  $\text{ClF}_3$  (Frame 23). The two axial Cl–F bonds clearly have a weaker covalent character than the equatorial bond, corresponding well to the canonical forms **10** and **11**.<sup>[13]</sup>

The core electron densities vanish if one uses a pseudo-potential method rather than performing all-electron calculations. We have done this in the case of Sn compounds, and therefore our representations of the Sn compounds exhibit no high electron densities around the nuclei but only the black background. The lone-pair electrons in  $\text{Sn}^{\text{II}}$  compounds are nicely illustrated by ELF. The spatial distribution of the lone pair in the  $\text{SnO}$  molecule (Frame 24) is clearly deformed and remarkably large. The  $\text{Sn}_2\text{O}_2$  dimer (Frame 25) shows a similarly expanded spatial distribution of these electron pairs and is an impressive indication of its stereochemical activity. Unlike their carbon analogues,  $\text{Sn}_2\text{R}_4$  molecules are not planar. The explanation involves the influence of the electron lone pairs.<sup>[14]</sup> For the bent  $\text{Sn}_2\text{H}_4$  molecule **12**, ELF actually shows a strong deformation (Frame 26), and the influence of the lone pairs is especially clear in comparison with the hypothetical planar structure of Frame 27. The large white region is intermediate between the case of two isolated lone pairs (as in Frame 25) and the case of a pure double bond (as in Frame 27).



The heterocubane cluster  $\text{Cu}_4\text{Sn}_4$  possesses an  $\text{Sn}_4$  tetrahedron. Here one finds multicenter bonding with participation of the Cu atoms. The plane depicted in Frame 28 contains an edge of the  $\text{Sn}_4$  tetrahedron (Frame 28 top, connecting the dark nuclear positions) and the middle of the opposite edge (Frame 28 bottom, middle of the yellow region). Two Cu atoms also lie in this plane (Frame 28 bottom, outer nuclear positions). Here again, the distribution of the Sn lone pairs is deformed.

In this first survey of the potential applications of the Electron Localization Function, ELF, we have demonstrated that notions such as atomic shells, chemical bonds, and lone electron pairs are readily manifested by a function that is based, in principle, on measurable physical quantities. Empirical findings, such as those expressed in the Gillespie–Nyholm rules, may be easily visualized thereby. Perhaps further investigations with the Electron Localization Function will prove beneficial in cases where classical concepts and chemical intuition fail.

- [1] W. England, L. S. Salmon, K. Ruedenberg, *Top. Curr. Chem.* 23 (1971) 31.
- [2] W. England, *Int. J. Quantum Chem.* 5 (1971) 683.
- [3] A. D. Becke, K. E. Edgecombe, *J. Chem. Phys.* 92 (1990) 5397.
- [4] J. E. Lennard-Jones, *J. Chem. Phys.* 20 (1952) 1024.
- [5] R. J. Gillespie, R. S. Nyholm, *Q. Rev.* 11 (1957) 339.
- [6] Details of the calculations: a) Basis sets: W. J. Hehre, R. Ditchfield, J. A. Pople, *J. Chem. Phys.* 56 (1972) 2257; P. C. Hariharan, J. A. Pople, *Theor. Chim. Acta* 28 (1973) 213; M. F. Frankl, W. J. Pietro, W. J. Hehre, J. S. Binkley, M. S. Gordon, D. J. Defrees, J. A. Pople, *J. Chem. Phys.* 77 (1982) 3654 (for **6–11**, ClF), G. Igel-Mann, C. Feller, H.-J. Flad, A. Savin, H. Stoll, H. Preuss, *Mol. Phys.* 68 (1989) 209 (for the Sn compounds); F. B. van Duijneveldt, *IBM Res. Rep.* 945 (1991) (contracted after G. C. Lie, E. Clementi, *J. Chem. Phys.* 60 (1974) 1275) (for all other compounds); b) Molecular Structures: K. P. Huber, G. Herzberg: *Molecular Spectra and Molecular Structures, Vol. 4*, Van Nostrand, New York 1979 (diatomic molecules); L. E. Sutton (ed.): *Tables of Interatomic Distances and Configurations in Molecules and Ions*, The Chemical Society, London 1958 (5–9 and  $\text{FHF}^{\ominus}$ ); I. Boustani, W. Pevestorf, P. Fantucci, V. Bonačić-Koutecký, J. Koutecký, *Phys. Rev. B* 25 (1987) 9437 (Li cluster); G. Igel-Mann, C. Feller, H.-J. Flad, A. Savin, H. Stoll, H. Preuss, *Mol. Phys.* 68 (1989) 209 (SnO); G. Igel-Mann, H.-J. Flad, C. Feller, H. Preuss, *J. Mol. Struct. (THEOCHEM)* 209 (1990) 313 ( $\text{Sn}_2\text{O}_2$ ); G. Trinquier, J. P. Malrieu, P. Riviere, *J. Am. Chem. Soc.* 104 (1982) 4529 (18); W. Plass, A. Savin, H. Stoll, H. Preuss, R. Nesper, H. G. von Schnering, *Inorg. Chem.* 29 (1990) 260 ( $\text{Cu}_4\text{Sn}_4$ ); c) SCF program: L. E. McMurchie, S. T. Elbert, S. R. Langhoff, E. R. Davidson: *Program MELD*, NRCC program QC04 (graciously supplied by Prof. Dr. E. R. Davidson); W. Meyer, P. Pulay, E. A. Reinsch, H. J. Werner: *Program MOLPRO* (graciously supplied by Prof. H. J. Werner); both programs were installed on the Cray-2 of the Computer Center of the Universität Stuttgart by Prof. H. Stoll, Dr. U. Wnig and B. Miehlich.
- [7] G. Igel-Mann, H. Stoll, H. Preuss, *Mol. Phys.* 65 (1988) 1321.
- [8] W. C. Clinton, J. Nakhleh, F. Wunderlich, *Phys. Rev.* 177 (1969) 1; W. C. Clinton, A. J. Galli, L. J. Massa, *ibid.* 177 (1969) 7; W. C. Clinton, G. A. Henderson, J. V. Prestia, *ibid.* 177 (1969) 13; W. C. Clinton, G. B. Lamers, *ibid.* 177 (1969) 19; W. C. Clinton, A. J. Galli, G. A. Henderson, G. B. Lamers, L. J. Massa, J. Zarur, *ibid.* 177 (1969) 27; W. C. Clinton, L. J. Massa, *Phys. Rev. Lett.* 29 (1972) 1363; R. F. Stewart, *J. Chem. Phys.* 51 (1969) 4569.
- [9] P. Coppens, T. V. Willoughby, L. N. Gonka, *Acta Crystallogr. Sect. A* 27 (1971) 248; W. H. E. Schwarz, B. Müller, *Chem. Phys. Lett.* 166 (1990) 621.
- [10] H. Schmider, V. H. Smith, Jr., W. Weyrich, *Trans. Am. Crystallogr. Assoc.* 26 (1991), in press.
- [11] J. Flad, F.-X. Fraschio, B. Miehlich: *Program GRAPA*, Institut für Theoretische Chemie der Universität Stuttgart, 1989.
- [12] H. E. White, *Phys. Rev.* 37 (1931) 1416.
- [13] W. Kutzelnigg: *Einführung in der Theoretische Chemie, Vol. 2*, Verlag Chemie, Weinheim, 375.
- [14] Compare D. E. Goldberg, P. B. Hitchcock, M. F. Lappert, K. M. Thomas, A. J. Thomas, T. Fjeldberg, A. Haaland, B. E. R. Schilling, *J. Chem. Soc. Dalton Trans.* 1986, 2387.

## Synthesis of a Biologically Active Taxol Analogue\*\*

By Siegfried Blechert\* and Andrea Kleine-Klausing

The taxanes from the plant family Taxaceae form a group of very unusual tricyclic diterpenes.<sup>[1]</sup> An eight-membered ring with two geminal methyl groups, an annulated six-membered ring, and a C3-bridge results in a strained half-spherical ring system, that has many oxygen functionalities. One of the most interesting members is taxol **1**,<sup>[2]</sup> which at present is being intensively studied as a promising chemotherapy agent for several types of tumors.<sup>[3]</sup> Till now it has remained the only known naturally occurring compound that accelerates the polymerization of tubulin and blocks its depolymer-

[\*] Prof. Dr. S. Blechert, A. Kleine-Klausing  
Institut für Organische Chemie der Technischen Universität  
Strasse des 17. Juni 135, W-1000 Berlin 12 (FRG)

[\*\*] This work was supported by the Deutsche Forschungsgemeinschaft and the Fonds der Chemischen Industrie.